periodica polytechnica

Mechanical Engineering
53/2 (2009) 87–92
doi: 10.3311/pp.me.2009-2.06
web: http://www.pp.bme.hu/me

RESEARCH ARTICLE

Modelling tooth-shape errors using random variables

István Groma / *Tibor* Bercsey

Received 2010-09-10

Abstract

The development of the industry consecutively requires more exact and more efficient power transmission techniques. In order to create efficiently meshing gears it is mandatory to manufacture the gears with accurate geometrical shape. This is especially true for worm gears in hypoid or in spiroid drives. Former approaches were focusing on the properties of geometrically ideal worm gears. Taking manufacturing limitations into account the ideal shape is not the case of real gears. The authors' indication is that these inaccuracies should not be neglected. Accordingly the goal of our study is to work out an adaptable mathematical approach for handling the shape errors of worm gears.

Keywords

tooth-shape errors · tooth grinding · random geometry · worm drive

Acknowledgement

The authors are grateful for the financial support of the Hungarian Scientific Research Fund (OTKA), Hungary, project No. K 62875.

István Groma
Department of Machine and Industrial Product Design, BME, H-1111 Budapest, Műegyetem rkp 1., Hungary
e-mail: groma.istvan@gt3.bme.hu

Tibor Bercsey
Department of Machine and Industrial Product Design, BME, H-1111 Budapest, Műegyetem rkp 1., Hungary
e-mail: bercsey.tibor@gt3.bme.hu

1 Introduction

Worm gears are used in several types of drive systems like bevel, spiroid and hypoid drives. A common way of manufacturing worm gears is by cutting one or more thread surfaces into a conical or cylindrical gear blank [6]. In a case when the worm is paired with a worm face gear, the teeth of the conjugate worm face gear can be cut using a miller constructed with the same manufacturing machine as the worm.

Based on the gear theory the geometry of a tooth may be studied in terms of differential geometry [3, 10]. It is reasonable to treat the flank as the enveloping surface of the manufacturing tool since the mathematical background is well elaborated.

Regarding meshing, the most important segment of the worm's geometry is the flank [7]. The goal is to describe the flank as the result of the manufacturing processes, more precisely the enveloping surface of the grinding wheel over its path. Accordingly a formal description of the flank can be achieved where the manufacturing parameters and settings (dimensions, angular velocity etc.) are the active variables.

Former approaches produced an explicit description for the flank, our approach results in a whole set of conceivable surfaces [3, 6, 10]. All dimensions and settings (hereafter manufacturing parameters) are taken as random variables. These stochastic variables do not provide an explicit geometry but a set of conceivable flank shapes.

Tooth-shape errors can generally be described as a flaw or an inaccuracy of some manufacturing parameters or as a fault of the material in use. This brings the suggestion to add uncertainty to these manufacturing parameters, thus it is expedient to model them with random variables. Although many types of distribution are conceivable for random variables, in our approach only the normal distribution is used (Gaussian random variable) since mainly physically measurable quantities are given. The properties of the distribution (mean, variance) can be obtained from measurement. It is clear that errors can have many different characteristics, thus a proper classification should be made regarding the types of errors.

1.1 Random error

It is obvious that there are manufacturing parameters which can only be measured with reasonable symmetric tolerance [1,2]

$$p \pm E. \tag{1}$$

Such parameters are represented by Gaussian random variables as follows

$$X \sim \Phi_{p,\frac{E}{3}}. \tag{2}$$

From measurement results the average and the standard deviation can be calculated and consequently the corresponding distribution as well.

If the deviation equals to zero then the cumulative distribution function of the random variable is the Heaviside step function denoting a constant distribution. In order to get back the description of the ideal geometry, it is possible to eliminate the error acting on a manufacturing parameter by substituting its deviation with zero.

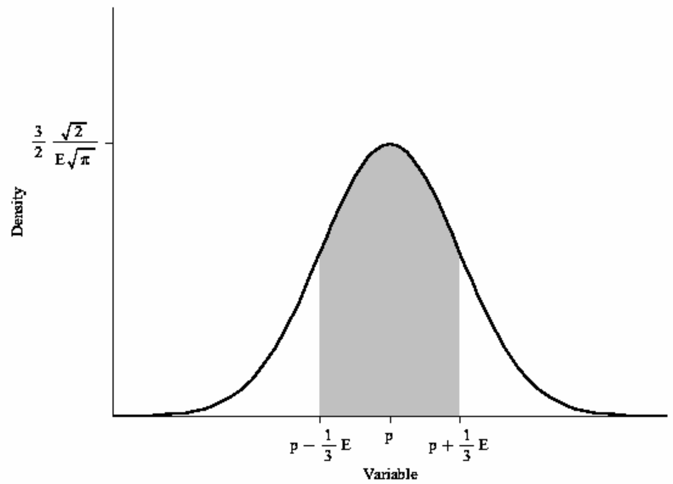

Fig. 1. Graph of a manufacturing parameter with Gaussian distribution.

1.2 Random noise

Random noise is a totally random, unavoidable noise on a manufacturing parameter without any history. It is understood that random noise has Gaussian amplitude distribution. Each infinitesimal moment during manufacturing can be interpreted as a Gaussian random variable. It is complicated to handle such a structure hence a discrete approach is preferred instead. The idea is to create a random sampling on a given time interval $[0, T]$. Each element of the population is a disjoint and a uniform Gaussian random variable where the mean is the average rate of the signal (s) and the variance is the square root of the average of the squared amplitudes of the noise (a)

$$\mu := s, \quad \sigma := \sqrt{a}. \tag{3}$$

On this sample an interpolation can be made (e.g. natural cubic spline interpolation) in order to have a continuous signal over the time interval reads as follows

$$RN\,[f;\mu;\sigma] := S_3\left(X_0, ..., X_{\lfloor fT \rfloor}\right) \text{ where } \forall i : X_i \approx \Phi_{\mu,\sigma}. \tag{4}$$

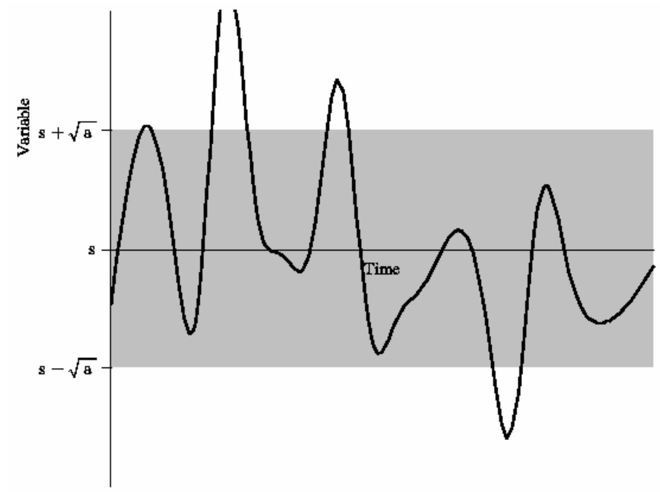

Fig. 2. Graph of a manufacturing parameter with random noise.

1.3 Unified formalism

In our approach all manufacturing parameters are represented as a random error or a random noise or both. In order to achieve a unique description for the manufacturing parameter the so-called RN-formalism was introduced. This way all variables are treated uniquely. Table 1 holds the adequate formalisation for common cases of error representation.

Tab. 1. Formalising different types of manufacturing parameters.

Type of manufacturing parameters	Formalism
A constant parameter with a real value p.	$RN\,[0;p;0]$
A measured parameter with a mean p and tolerance E.	$RN\left[0;p;\frac{E}{3}\right]$
A random noise with signal s, amplitude a and a sampling frequency f.	$RN\left[f;s;\sqrt{a}\right]$
A random noise with uncertain signal s, tolerance E, amplitude a and sampling frequency f.	$RN\left[0;s;\frac{E}{3}\right]+$ $+RN\left[f;0;\sqrt{a}\right]$

There is another advantage of this formalism: all manufacturing parameters can be substituted by values of Gaussian random variables (see Fig. 3). Thus the varying geometry depends only on a finite set of likewise random variables.

1.4 Random geometry

Let us consider that the tooth-shape is given by a continuous transformation mapping a strip and the manufacturing parameters into a 3-dimension space as follows [10]

$$\vec{H} : D \to R^3. \tag{5}$$

In Eq. (5) D is a domain consisting of two technical variables for surface description and the space of the manufacturing parameters. The relations between manufacturing parameters and imperative constraints – like all lengths must be positive, the tooth must fit to the gear blank etc. – are described by the domain. The domain has to include all practical configurations. The basic idea of our approach is to substitute the manufacturing parameters with the RN-formalism in order to get the distribution of tooth-shapes. Thus in place of a particular tooth surface a set of conceivable tooth-shapes was formalised a so-called random geometry [5, 8].

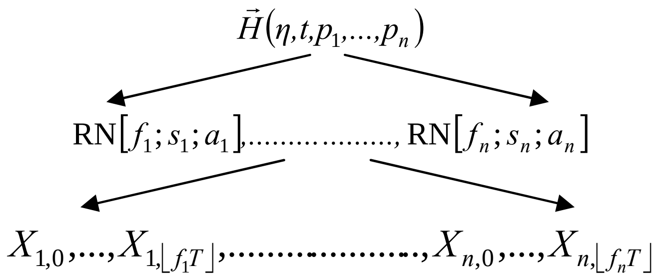

Fig. 3. The evaluation process for substituting errors into the geometry.

2 Application

In order to model tooth-shape errors for worms the geometry of the flank has to be described as a surface mapping. The flank in the case of worms is a thread surface where the profile of the thread is conjugate to the geometry of the cutting tool. Assume that the teeth are manufactured by grinding process so the initial step is to formulate the cutting surface of the grinding wheel. We assume that the profile can be described as mapping a real parameter ψ to a continuous plane curve (regular curve) [3]. A rectangular coordinate system (R2) with homogeneous coordinates is used where the origin is at the centre of the wheel.

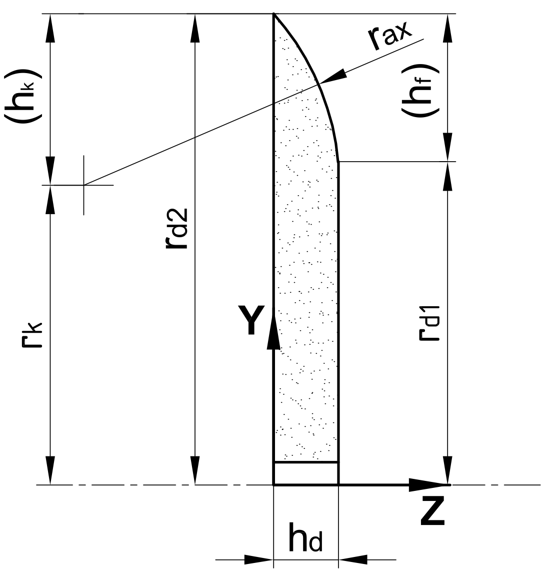

Fig. 4. Axial section of the grinding wheel.

The axial section of the grinding wheel on plane YZ is shown on Fig. 4. By rotating the edge curve around axis Z – introducing another technical parameter η – the final surface is achieved as follows

$$r(\eta) := \sqrt{h_k^2 - 2\sqrt{r_{ax}^2 - h_k^2}\,\eta - \eta^2} - h_k + h_f + r_{d1}, \qquad (6)$$

$$\vec{r}_{R2}(\eta,\psi) := \begin{pmatrix} \sin(\psi)\, r(\eta) \\ \cos(\psi)\, r(\eta) \\ \eta \\ 1 \end{pmatrix}. \qquad (7)$$

The motion of both the grinding wheel and the gear blank can be described in different coordinate systems. For practical reasons we are interested in the motion of a grinding wheel relative to the gear blank [6, 10]. This motion is decomposed into several elementary motions (like rotation, translation etc.). If homogeneous coordinates are applied these motions are linear transformations, thus they can be represented by matrices [5]

$$M_{2,R2}(t) := \begin{bmatrix} C_{\omega_2} & S_{\omega_2} & 0 & 0 \\ -S_{\omega_2} & C_{\omega_2} & 0 & 0 \\ 0 & 0 & 1 & 0 \\ 0 & 0 & 0 & 1 \end{bmatrix}, \qquad (8)$$

$$M_{T1,2}(t) := \begin{bmatrix} 1 & 0 & 0 & 0 \\ 0 & C_\delta & -S_\delta & 0 \\ 0 & S_\delta & C_\delta & 0 \\ 0 & 0 & 0 & 1 \end{bmatrix}, \qquad (9)$$

$$M_{T2,T1}(t) := \begin{bmatrix} C_\Gamma & 0 & -S_\Gamma & 0 \\ 0 & 1 & 0 & 0 \\ S_\Gamma & 0 & C_\Gamma & 0 \\ 0 & 0 & 0 & 1 \end{bmatrix}, \qquad (10)$$

$$M_{T3,T2}(t) := \begin{bmatrix} 1 & 0 & 0 & x_0 \\ 0 & 1 & 0 & -y_0 \\ 0 & 0 & 1 & -z_0 \\ 0 & 0 & 0 & 1 \end{bmatrix}, \qquad (11)$$

$$M_{1,T3}(t) := \begin{bmatrix} 1 & 0 & 0 & 0 \\ 0 & 1 & 0 & -D_{v_r} \\ 0 & 0 & 1 & D_{v_{ax}} \\ 0 & 0 & 0 & 1 \end{bmatrix}, \qquad (12)$$

$$M_{R1,1}(t) := \begin{bmatrix} C_{\omega_1} & S_{\omega_1} & 0 & 0 \\ -S_{\omega_1} & C_{\omega_1} & 0 & 0 \\ 0 & 0 & 1 & 0 \\ 0 & 0 & 0 & 1 \end{bmatrix}. \qquad (13)$$

Each matrix represents a basic motion or a coordinate system change as indicated on Fig. 5. The final matrix for changing from the coordinate system of the grinding wheel to the coordinate system of the gear blank is

$$M_{R1,R2} := M_{R1,1} M_{1,T3} M_{T3,T2} M_{T2,T1} M_{T1,2} M_{2,R2}. \qquad (14)$$

The description of the enveloping surface can be found by ap-

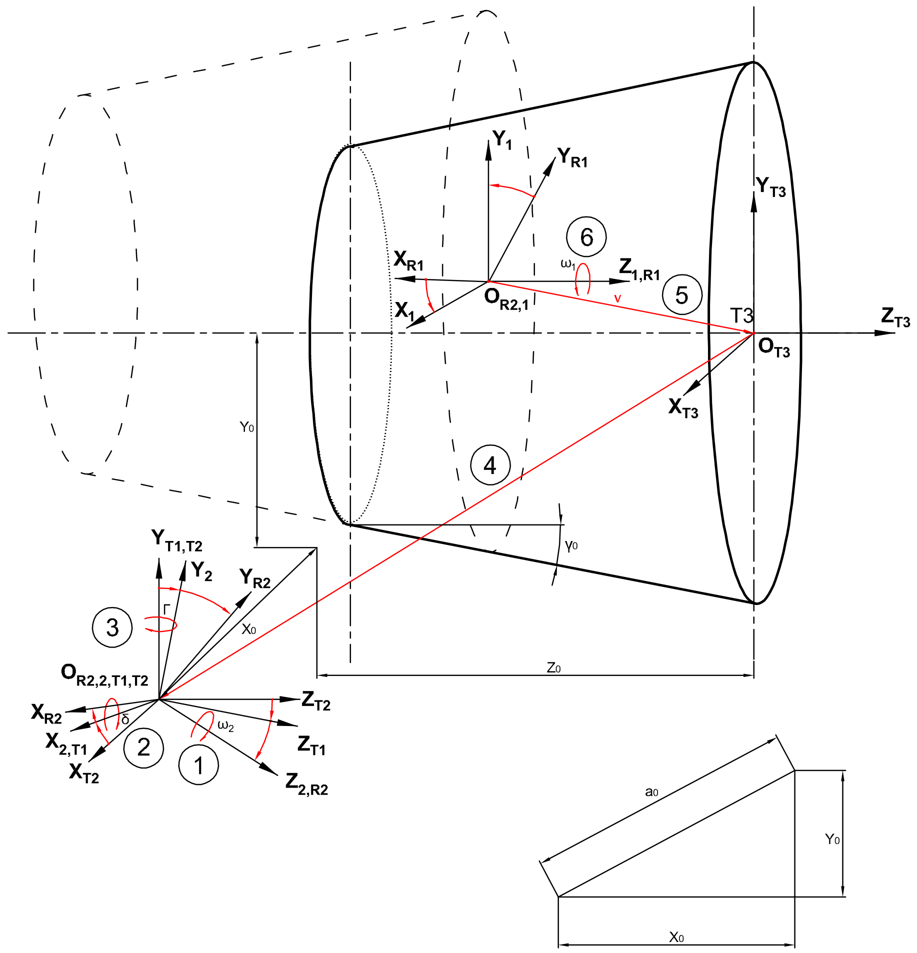

Fig. 5. The elementary motion components of the grinding wheel's path.

Tab. 2. Short description of decomposed elementary motions.

Nr.	Elementary motion
1	Axial rotation of the grinding wheel ($M_{2,R2}$).
2	Tilting the grinding wheel into profile ($M_{T1,2}$).
3	Rotating the grinding wheel to lead angle ($M_{T2,T1}$).
4	Changing from the grinding position to the centre of the gear blank's face ($M_{T3,T2}$).
5	Shifting motion of the gear blank ($M_{1,T3}$).
6	Axial rotation of the gear blank ($M_{R1,1}$).

plying the first law of connection (13)

$$\vec{n}_{R1}\vec{v}^{(2)}_{R1} = \left(\frac{\partial \vec{r}_{R2}}{\partial \psi}(\eta,\psi) \times \frac{\partial \vec{r}_{R2}}{\partial \eta}(\eta,\psi)\right)^T \cdot$$
$$\cdot M^T_{R1,R2}(t)\,\frac{\partial M_{R1,R2}}{\partial t}(t)\,\vec{r}_{R2}(\eta,\psi) = 0. \quad (15)$$

This law is valid for any arbitrary point on the surface and states that the relative velocity is perpendicular to the normal vector of the enveloping and the generating surface as well. In the particular case of flanks one can find that a parameter can be expressed from Eq. (15) like

$$\Psi(\eta,t) := \min_{\|E_{XY}\vec{r}_{R1}(\eta,\psi,t)\|_2} \left\{ \psi \,\middle|\, \vec{n}_{R1}(\eta,\psi,t)\,\vec{v}^{(2)}_{R1}(\eta,\psi,t) = 0 \right\}. \quad (16)$$

It should be mentioned that the first law of connection yields two solutions but only one of them belongs to the internal volume of the gear blank. This can obviously be stated by the relation as follows

$$\|E_{XY}\vec{r}_{R1}(\eta,t)\|_2 \le r - v_r t. \quad (17)$$

Summarising these results the mapping for the flank of the worm reads as

$$\vec{H}(\eta,t,r_{ax},h_k,h_f,r,h,\Gamma,\delta,x_0,y_0,z_0,v_{ax},v_r,\omega_1,\omega_2)$$
$$:= \vec{r}_{1R}(\eta,t) = M_{R1,R2}(t)\,\vec{r}_{R2}(\eta,t)\,. \quad (18)$$

In Eq. (18) we have the mapping which is appropriate for extending with the RN-formalism like on Fig. 3. This is the step where error modelling is introduced in the model, replacing constant manufacturing parameters with corresponding random errors and random noises.

Random geometry is actually a continuous set containing all conceivable geometries with a probability measure. Due to the difficulties of the subject, a random geometry cannot be examined directly. Our suggestion is to consider the set as a population, hence statistical tools and techniques can be used for analysis. In order to find some properties of the flank a sufficient quantity of samples is required. To choose a suitable cardinality for the sample the following expression is applicable:

$$|\text{Sample}| \geq \prod_i \left\lfloor Z \left(\frac{\sigma_i}{ME} \right)^2 + 1 \right\rfloor, \quad \Phi_{0,1}(Z) = 1 - \frac{\alpha}{2}. \quad (19)$$

The elements of the sample are definite surface geometries and for instance, proper CAD models can be driven from them. Of course, this needs some software support. A computer program was developed to create a random sample of the manufacturing parameters (see Fig. 6). From each element of the sample the appropriate tooth surface can be computed and it is possible to carry out a Monte Carlo algorithm style analysis.

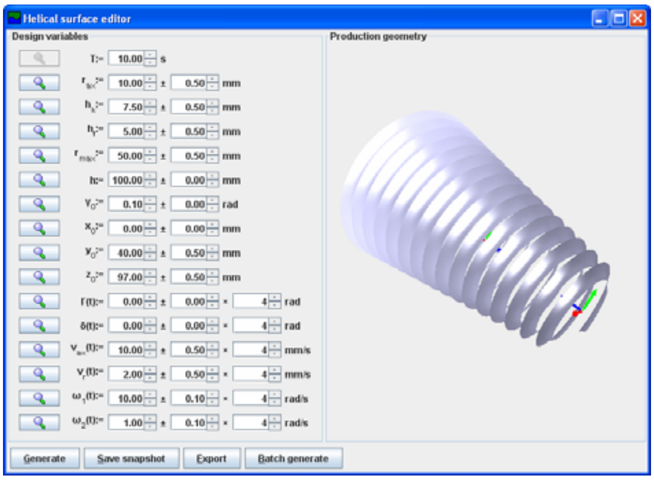

Fig. 6. A screen shot from the software for computing statistical calculations about the tooth surface's geometry.

3 Case study

In order to demonstrate the advantages of our approach we conducted some experiments on spur gears. The test gears have involute tooth profile, their specification is the following:

$$\begin{aligned} z &= 9, \\ m &= 5, \\ \varphi &= 20^\circ, \\ x &= +0.069, \\ h_t &= 12.65\text{mm}, \\ D_b &= 42.286\text{mm}. \end{aligned}$$

The whole group was manufactured on the same Niles ZSTZ 315 C1 gear grinder. A span measurement was carried out on all 9 teeth of 40 test gears. After summarising the data we recorded that the average span measure over 2 teeth is 22.8670mm and the variance on the sample is $7.1238 \cdot 10^{-5}$.

It is practicable to describe the flank as a surface mapping but in order to keep the study simple the span measure was calculated directly pending on two manufacturing parameters (pressure angle and profile shift) [4]

$$W_k(\varphi, x') = m \cos(\varphi) \left[\left(k - \frac{1}{2} \right) \pi + z_{\text{inv}}(\varphi) \right] + 2x' \sin(\varphi). \quad (20)$$

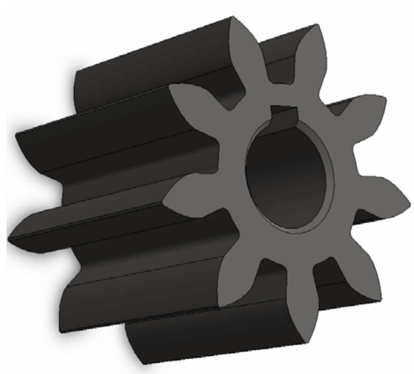

Fig. 7. CAD model of the test spur gear.

Both of the manufacturing parameters in Eq. (20) have some reasonable tolerance which should be taken into account for a better description of properties of the spur gears. With some estimated tolerances for the manufacturing parameters the RN-formalism reads as follows:

$$W_2 \left(RN \left[0; 20^\circ + 2^\circ; \frac{1^\circ}{3} \right], \right. \\ \left. RN \left[0; 0.345\text{mm} + 0.095\text{mm}; \frac{0.1\text{mm}}{3} \right] \right). \quad (21)$$

Eq. (21) was evaluated over 50 000 random instances and it produced data for W_2 with an average of 22.8705mm and a variance $7.4606 \cdot 10^{-5}$. If the measured and computed data is compared to each other we find a significant similarity by means of statistical features. Nevertheless, comparing the estimated and the real error boundaries of the manufacturing parameters remains for future examinations.

4 Conclusions

In the case of meshing gears the properties of motion transmission is essentially influenced by the shape of the tooth. The use of fine teeth results in smaller energy loss. Energy loss may lead to unpleasant effects like noise, physical wear and can heavily exhaust the bearings, too. Because of physical limitations, the tooth-shape cannot be manufactured with an ideal geometry. In order to handle shape errors a random geometry was introduced for the tooth surface. With the random geometry, the flaws and inaccuracies of a real manufacturing process can be described. As a result, one is able to examine the arbitrary properties of worm gear's shape (e.g. the behaviour of lubrication fluid [9]) with statistical analysis. Our approach is applicable with a software system that can create random samplings from a shape population for several types of examination. With this model, product quality characteristics and requirements on manufacturing process can be obtained.

Nomenclature

α	Significance level.
C_δ	$:= \cos(\delta(t))$
C_Γ	$:= \cos(\Gamma(t))$
C_{ω_1}	$:= \cos\left(\int_0^t \omega_1(t)\,dt\right)$
C_{ω_2}	$:= \cos\left(\int_0^t \omega_2(t)\,dt\right)$
D	Domain of tooth surface mapping.
D_b	Diameter of base circle of the test spur gear.
D_{υ_r}	$:= \int_0^t \upsilon_r(t)\,dt$
$D_{\upsilon_{ax}}$	$:= \int_0^t \upsilon_{ax}(t)\,dt$
$\delta(t)$	Tilting angle of wheel into profile of helical surface.
E_{XY}	Projection matrix to plane X-Y.
φ	Pressure angle of the test spur gear.
$\Phi_{\mu,\sigma}(x)$	$:= \frac{1}{\sigma\sqrt{2\pi}} \int_{-\infty}^{x} e^{-\frac{(z-\mu)^2}{2\sigma^2}}\,dz$
$\Gamma(t)$	Lead angle on the worm's reference angle.
h	The length of the conical piece.
h_f	The actual depth of the tooth.
h_k	The distance between centre of the edge circle and the bottom of the tooth.
h_t	Whole tooth depth of the test spur gear.
η	$\in \left[0, \sqrt{r_{ax}^2 - h_k^2 + 2h_k h_f - h_f^2} - \sqrt{r_{ax}^2 - h_k^2}\right]$
m	Module of the test spur gear.
ME	Margin of statistical error.
r	The maximal radius of the conical piece.
r_{d1}	The minimal radius of the grinding wheel.
r_a	Radius of base circle of the test spur gear.
r_{ax}	The radius of the edge circle.
$S_3(\ldots)$	Natural cubic spline over finite set of points.
S_δ	$:= \sin(\delta(t))$
S_Γ	$:= \sin(\Gamma(t))$
S_{ω_1}	$:= \sin\left(\int_0^t \omega_1(t)\,dt\right)$
S_{ω_2}	$:= \sin\left(\int_0^t \omega_2(t)\,dt\right)$
$\upsilon_{ax}(t)$	The shifting velocity of the grinding wheel in axial direction.
$\upsilon_r(t)$	The shifting velocity of the grinding wheel in radial direction.
W_k	Span measure over k teeth of the test spur gear.
$\omega_1(t)$	Angular velocity of the manufactured piece.
$\omega_2(t)$	Angular velocity of the grinding wheel.
x	Profile shift coefficient of the test spur gear.
x'	$:= mx$
z	Number of teeth on the test spur gear.
x_0, y_0, z_0	The coordinates of the starting offset of the grinding wheel relative to the blank.
ψ	$\in [0, 2\pi]$

References

1 *DIN 3974-1: Accuracy of worms and worm gears - Part 1: General bases*, 1995.

2 *DIN 3974-2: Accuracy of worms and worm gears - Part 2: Tolerances for individual errors*, 1995.

3 **Litvin F L, Fuentes A**, *Gear Geometry and Applied Theory*, Cambridge University Press, Cambridge, 2004.

4 **Steinhilper W, Sauer B**, *Konstruktionselemente des Maschinenbaus 2*, Springer, Berlin, 2006.

5 **Bercsey T, Groma I**, *Modeling shape errors of worm gears*, 2007 ASME International Design Engineering Technical Conferences and Computers and Information in Engineering Conference, 2007.

6 **Dudás I**, *The Theory and Practice of Worm Gear Drives*, Page US, Sterling, 2004.

7 **Szeniczei L**, *Csigahajtóművek*, Műszaki könyvkiadó, Budapest, 1957.

8 **Bercsey T, Groma I, Horák P**, *Modeling errors in worm gear manufacturing with random variables.*, Dresdner Maschinenelemente Kolloquium, 2007, pp. 171–182.

9 **Bercsey T, Horák P**, *Analyse der Schmierungsverhältnisse und Abweichungen von ZTA-Schneckengetrieben*, Dresdner Maschinenelemente Kolloquium, 2005, pp. 209–218.

10 **Balajti Zs**, *Development of the Production Geometry of Kinematic Drive Pairs*, 2007. PhD thesis.